

# Radio-echo sounding and ice volume estimates of western Nordenskiöld Land glaciers, Svalbard

A. MARTÍN-ESPAÑOL,<sup>1</sup> E.V. VASILENKO,<sup>2</sup> F.J. NAVARRO,<sup>1</sup> J. OTERO,<sup>1</sup>  
J.J. LAPAZARAN,<sup>1</sup> I. LAVRENTIEV,<sup>3</sup> Y.Y. MACHERET,<sup>3</sup> F. MACHÍO<sup>4</sup>

<sup>1</sup>Department of Applied Mathematics, Technical University of Madrid, Madrid, Spain  
E-mail: alba.mespanol@upm.es

<sup>2</sup>Institute of Industrial Research Akademribor, Academy of Sciences of Uzbekistan, Tashkent, Uzbekistan

<sup>3</sup>Institute of Geography, Russian Academy of Sciences, Moscow, Russia

<sup>4</sup>Escuela Superior de Ingeniería y Arquitectura, Universidad Pontificia de Salamanca en Madrid/Fundación Pablo VI, Madrid, Spain

**ABSTRACT.** As part of ongoing work to obtain a reliable estimate of the total ice volume of Svalbard glaciers and their potential contribution to sea-level rise, we present here volume calculations, with detailed error estimates, for ten glaciers on western Nordenskiöld Land, central Spitsbergen, Svalbard. The volume estimates are based upon a dense net of GPR-retrieved ice thickness data collected over several field campaigns spanning the period 1999–2012. The total area and volume of the ensemble are  $116.06 \pm 4.53 \text{ km}^2$  and  $10.439 \pm 0.373 \text{ km}^3$ , respectively, while the individual areas, volumes and average ice thickness lie within 2.6–50.4 km<sup>2</sup>, 0.08–5.54 km<sup>3</sup> and 29–108 m, respectively. Volume/area scaling relationships overestimate the total volume of these glaciers by up to 35% with respect to our calculation. On the basis of the pattern of scattering in the radargrams, we also analyse the hydrothermal structure of these glaciers. Nine of the ten are polythermal, while only one is entirely cold.

## INTRODUCTION

Mountain glaciers and ice caps (GICs) are important contributors to current sea-level rise (SLR) (Solomon and others, 2007) and are likely to continue to be so during the 21st century (Radić and Hock, 2011), in spite of the growing contribution from the ice sheets of Greenland and Antarctica (Rignot and others, 2011). For how long, and to what extent, GICs will contribute to SLR depends on their total ice volume, which is not accurately known because of the scarcity of direct observations of glacier ice thickness. Because of this, the global estimates of the volume of GICs are based on either volume/area scaling relationships (Radić and Hock, 2010; Grinsted, 2013) or on simple physically based approaches relating thickness distribution to glacier geometry and dynamics (Huss and Farinotti, 2012). Their estimates, however, vary considerably.

Svalbard, situated in the Atlantic sector of the Arctic (76–81° N, 10–33° E), is highly vulnerable to climate change (Hagen and others, 2003). Even though Svalbard is among the best-studied sectors of the Arctic, ice thickness measurements are only available for selected glaciers. The estimates of the total ice volume of Svalbard glaciers are therefore based on the scaling or physically based approaches mentioned above, or on empirical relationships specific to Svalbard glaciers, derived from the scarce and limited-accuracy ice thickness measurements that were available in the early 1980s (Macheret and Zhuravlev, 1982) and the early 1990s (Hagen and others, 1993).

The results presented in this paper are part of ongoing work within the ‘Sensitivity of Svalbard glaciers to climate change’ (SvalGlac) project. One of its major objectives is to obtain a reliable estimate of the total ice volume of Svalbard glaciers by deriving a new volume/area relationship specific to Svalbard glaciers, based on accurate ice volume estimates from ground-penetrating radar (GPR) data. Here we use GPR

data collected during several field campaigns within the period 1999–2012 to calculate the ice volume of ten glaciers in western Nordenskiöld Land, central Spitsbergen, Svalbard (Fig. 1), together with associated error estimates. This estimation involves compound errors from different sources, which often are not properly quantified in the literature. In addition to the volume estimates, this paper provides an insight into how to deal with error estimates when computing glacier volume from GPR-retrieved ice thickness data.

## FIELD DATA

The GPR data used in this study correspond to ten glaciers in Nordenskiöld Land, collected during several field campaigns between 1999 and 2012, all of them carried out during early spring, before the onset of strong surface melting. The different types of radar equipment, with their central frequency and the total length of radio-echo sounding (RES) profiles, are summarized in Table 1. The layout of GPR profiles is displayed in Figure 1, which also includes the 2007 glacier boundaries (Arendt and others, 2012; König and others, in press), modified using Landsat images to match the area at the time when the glaciers were echo sounded. For the profiling, transmitting and receiving antennas were arranged coaxially along the profiling direction (parallel end-fire), to minimize direct coupling between antennas and also the reflections from the glacier side-walls, as most of the profiles were transverse to the glacier centre line (Navarro and Eisen, 2010).

## METHODS

### GPR data processing

The radar data were processed using the commercial software packages RadExPro, by GDS Production (Kulnitsky and others, 2000), and ReflexW (<http://www.sandmeier-geo.de/>),

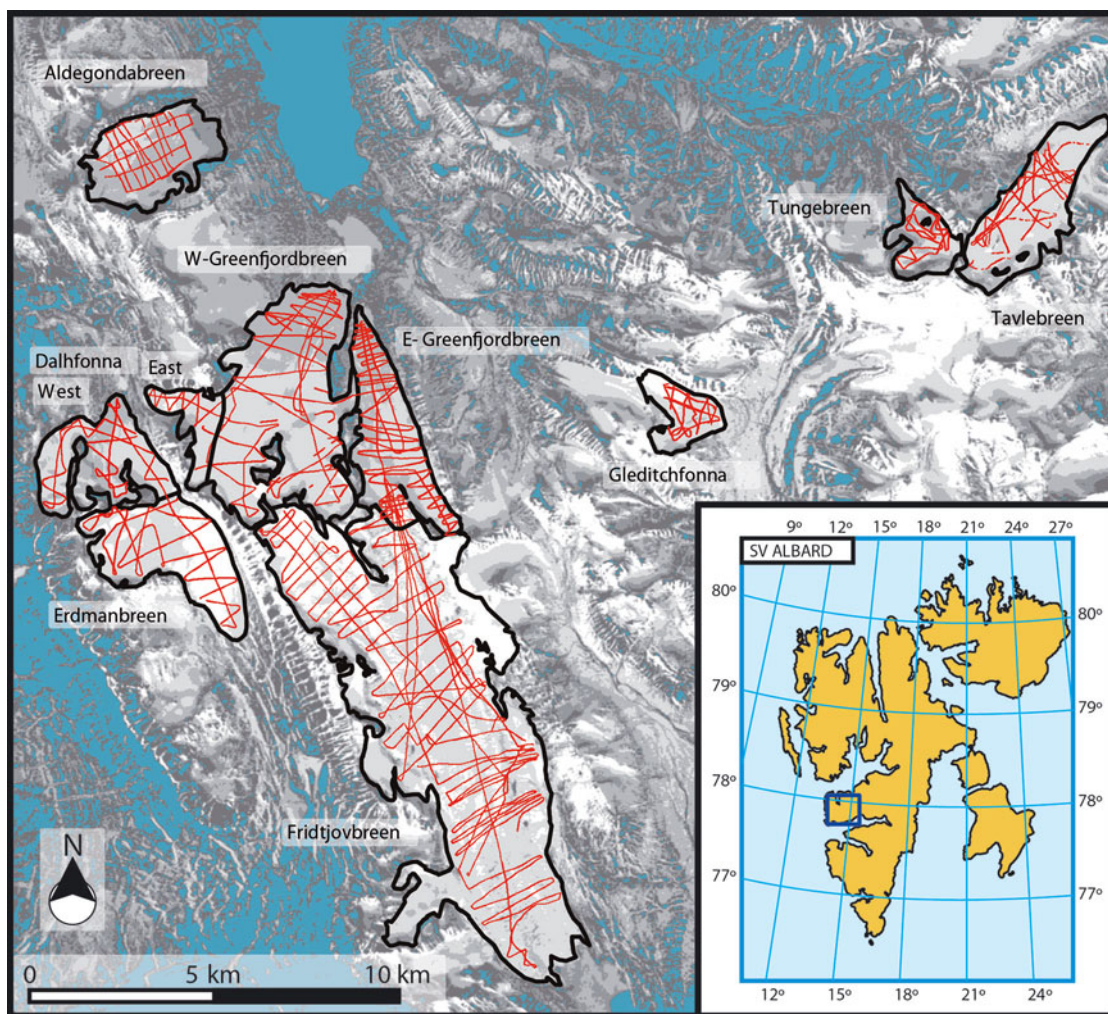


Fig. 1. Location of the studied glaciers and layout of GPR profiles.

and the main processing steps consisted of bandpass filtering, amplitude correction, deconvolution and migration. For the time-to-depth conversion we used a constant radio-wave velocity (RWV) of  $170 \text{ m } \mu\text{s}^{-1}$ . This RWV value was chosen on the basis of our own measurements by the common-midpoint (CMP) method (Macheret and others, 1993) on glaciers in this region (Navarro and others, 2005; Vasilenko and others, 2006) or in neighbouring regions in

Svalbard (Jania and others, 2005), carried out during early spring. Such a high RWV is typical of measurements made before the onset of strong melting; measurements made during warmer periods have substantially lower RWVs, due to the increased water content in temperate ice. A RWV of  $170 \text{ m } \mu\text{s}^{-1}$  has also been used in other GPR studies in Svalbard (Bælum and Benn, 2011; Saintenoy and others, 2013).

Table 1. GPR surveys. Ramac/GPR is manufactured by Malå Geoscience. VIRL2, VIRL6 and VIRL7 are GPR systems made in-house (described by Vasilenko and others, 2002; Berikashvili and others, 2006, and Vasilenko and others, 2011, respectively)

Glacier	Year	Equipment	Central frequency	Profile length
			MHz	km
Aldegondabreen	1999	VIRL2	15	40.0
Tavlebreen	2010	Ramac/GPR and VIRL6-VIRL7	20, 100 and 200	33.5
Austre Dahlfonna	2010	VIRL6	20	7.6
Austre Grønfjordbreen	2010	VIRL6	20	53.0
Vestre Grønfjordbreen	2010	Ramac/GPR and VIRL6	100 and 20	102.0
Gleditchfonna	2011	VIRL6	20	16.9
Tungebreen	2011	VIRL6	20	12.5
Vestre Dahlfonna	2012	VIRL6	20	25.7
Erdmanbreen	2012	VIRL6	20	31.2
Fridtjovbreen	2012	VIRL6 and VIRL7	20	180.0



## Data consistency

To properly interpolate a continuous surface from point data a coherent (self-consistent) source dataset is required. Crossover analysis is used to assess both internal accuracy and consistency between datasets (Bamber and others, 2001). Since all data contain errors, the ice thickness values measured at any crossover point will, in general, be different for the two intersecting radar lines. The value and spatial distribution of the crossover errors provide insight into the magnitude and source of the errors in the data (Retzlaff and others, 1993). Differences at the crossover points can be caused by inaccurate positioning of the data, picking errors or lack of (or improper) migration of any of the intervening profiles. In our analysis, the highest crossover differences appeared for crossovers involving radar profiles parallel and close to steep valley side-walls. In such cases, the radar often receives reflections from (and perpendicular to) the slopes of the valley walls rather than from the point underneath the radar position. The standard migration procedure only corrects the ice thickness for bed slope along the profiling direction. Consequently, it works properly for profiles perpendicular to the side-walls, but not for profiles parallel to them, and hence a large difference often appears at such crossovers. To avoid these problems, we discarded profiles parallel and close to the side-walls.

The ice thickness maps were constructed assuming that: (1) the ice thickness is zero at the lateral margins of the glacier, at the glacier front of land-terminating glaciers and at the contact points with nunataks; (2) if no thickness measurements are available at the other side of an ice divide, the ice thickness at the divide is extrapolated by a second-degree polynomial passing through three selected measurement points close to the divide and roughly aligned in the longitudinal (glacier-flow) direction; (3) the ice thickness near the valley side-walls decreases parabolically to zero at the side-wall along the direction perpendicular to it; and (4) the ice thickness near the front of land-terminating glaciers decreases linearly to zero at the front, a reasonable assumption for receding land-terminating glaciers (Cuffey and Paterson, 2010), such as those in this study (with the exception of Fridtjovbreen).

## Interpolation

Ice thickness measurements were interpolated into a regular grid using the Gridfit routine (D'Errico, 2006), available for MATLAB. This method has the capability to work with sparse or irregular data, and finds a smooth surface that is consistent with the data. This approach is better than implementing smoothing after interpolation, where smoothing is disconnected from the data. Gridfit uses an approximation method closely related to thin plate splines approximation, as opposed to interpolation, so that it is robust against noise and outliers (Bohorquez and Darby, 2008). The Gridfit routine has different user-selectable options, such as the interpolation method, the smoothing factor or the regularization method. We used the triangular interpolation method, leaving the default values for the remaining parameters. Further details about the algorithms used by Gridfit and its efficiency can be found at MATLAB Central File Exchange (D'Errico, 2006).

## Volume calculation in brief

The procedure we followed to derive the glacier volumes consisted of the following steps. (1) Collecting a coherent

GPR dataset, as discussed above. (2) Processing of GPR data following the methodology described above. (3) Calculating ice depths along the profile at  $\sim 1.5$  m intervals. (4) Interpolating the data into a regular grid using MATLAB. (5) Adjusting the 2007 glacier boundaries (Arendt and others, 2012; König and others, in press) to the year of the RES using Landsat images (this and the following step were performed using ArcGIS v9.3). (6) Clipping the resulting regular grid to the glacier boundary to build the final ice thickness map for each glacier. (7) Calculating the glacier volume, summing up every gridcell thickness value multiplied by the gridcell area.

## Error in volume estimate

We attempt to estimate the error in volume, using error propagation, from the separate error estimates for its main components. Errors in ice thickness and errors in area can be considered independent of each other, so their combined effect is approximated by root-mean-square (rms) summation

### Measurement error

The measurement error encompasses errors inherent to the ice thickness measurements using GPR (GPR errors) and errors due to inaccurate GPS positioning (GPS errors). We assume that all ice thickness data are affected by random errors. GPR errors encompass both instrumental errors and data-processing errors. The instrumental errors include the range resolution (which depends on the radar frequency) and the data-digitalization error (which depends on the sampling frequency). The range resolution is not an error in itself, but acts as a lower bound for the thickness measurement error. The data-processing errors include, among others, those related to lack of (or improper) migration, improper bed reflection picking or the errors incurred by the assumptions in the time-to-depth conversion (e.g. constant RWV). We assume that picking errors are negligible compared to the other errors. To estimate the GPR measurement error we followed the technique described by Navarro and Eisen (2010), which takes the error in two-way travel time as the inverse of the central frequency of the radar system, and assumes a typical relative error in RWV of  $\sim 2\%$ .

Stand-alone GPS systems were used for positioning. For the field surveys carried out after 2000, a typical accuracy of 5 m in horizontal positioning can be assumed (Sharma and Banerjee, 2009). However, for the 1999 echo sounding on Aldegondabreen the accuracy of the GPS horizontal positioning is expected to be much lower (errors of up to 100 m) (Parkinson and others, 1996). To estimate how much thickness change could be expected from inaccuracies in the horizontal positioning, we built a small-scale experimental variogram, assessing the thickness differences between measurement points separated by a distance equal to the GPS precision (100 m for Aldegondabreen, 5 m for the other glaciers). This quantifies the thickness error incurred by assigning to a given point the ice thickness corresponding to a different position, due to inaccurate GPS horizontal positioning. This difference will be larger in zones of steep bedrock.

### Interpolation error

GPR data are usually anisotropically distributed over the glacier surface, densely sampled along the radar tracks but widely spaced between distinct tracks. Well-known methods, such as cross-validation or jack-knifing techniques

**Table 2.** Estimated area based on the boundaries of the Randolph Glacier Inventory (RGI), volume, average thickness and maximum thickness for each glacier, with their estimated errors, and main components of the error in ice thickness

Glacier	Year	Area	$\epsilon_A$	Volume	$\epsilon_V$	$\epsilon_V/V$	$H_{\text{mean}}$	$H_{\text{max}}$	$\epsilon_{\text{GPS}}$	$\epsilon_{\text{GPR}}$	$\epsilon_{\text{Interp}}$
		km <sup>2</sup>	km <sup>2</sup>	km <sup>3</sup>	km <sup>3</sup>	%	m	m	m	m	m
Aldegondabreen	1999	7.18	0.57	0.469	0.053	11.3	68 ± 1	191 ± 25	14.2	5.8	7.0
Austre Dahlfonna	2010	2.56	0.20	0.181	0.013	7.0	99 ± 1	189 ± 5	0.9	5.0	8.6
Vestre Dahlfonna	2012	6.92	0.55	0.249	0.022	11.1	36 ± 1	151 ± 6	3.9	4.4	10.0
Erdmanbreen	2012	8.96	0.72	0.842	0.049	5.8	96 ± 1	190 ± 5	2.5	4.7	10.6
Fridtjovbreen	2012	50.37	4.03	5.542	0.330	5.9	108 ± 1	265 ± 16	8.8	5.2	18.6
Gleditchfonna	2011	2.76	0.22	0.076	0.006	7.5	29 ± 1	64 ± 5	1.9	4.3	5.2
Austre Grønfjordbreen	2010	8.31	0.67	0.637	0.033	5.25	79 ± 1	162 ± 5	1.7	5.8	7.0
Vestre Grønfjordbreen	2010	18.08	1.45	1.918	0.146	7.6	107 ± 1	215 ± 5	1.4	4.8	20.4
Tavlebreen	2010	8.04	0.64	0.440	0.040	9.0	55 ± 1	128 ± 3	1.1	3.1	15.7
Tungebreen	2011	2.88	0.23	0.086	0.005	5.8	32 ± 1	88 ± 5	1.4	4.3	6.5
Total		116.06	4.53	10.439	0.373	3.6					

(Davis, 1987; Isaaks and Srivastava, 1989), have often been used to quantify the accuracy of surface interpolation algorithms. However, these errors are not good estimators of the interpolation error when dealing with GPR-like data, because of their sparse and uneven distribution. Errors will not be representative for the glacier areas not covered by GPR profiles. Our method calculates an average interpolation error following the rationale of cross-validation techniques, but taking into account the variance of the error with the distance to the nearest neighbour. We first construct a function relating the interpolation error at any given point to the distance to the nearest GPR-measured data point, and then calculate a glacier-wide interpolation error by averaging the interpolation errors computed at each gridpoint.

#### Error in area

The error in area has two main sources: the uncertainty in identifying the boundary of the glacier (which we will refer to as uncertainty in boundary delineation) and, once a given boundary has been assumed, the error incurred in fitting the glacier boundary to the regular grid (which we will denote pixelation error). The uncertainty in boundary delineation arises from the overestimation of the area in the accumulation zone, due to snow-covered terrain, and the underestimation incurred in the ablation zone when glacier ice near the margins is covered by debris. In our study area, debris cover is fairly common, taking into account that most of the glaciers are small land-terminating mountain glaciers with steep valley walls. To account for the uncertainty in boundary delineation we have assumed an error in area of 8%, typical of glacier inventories for this region (personal communication from C. Nuth, 2013). The pixelation error has a negligible impact on the volume computation compared with the boundary delineation error assumed in this study.

## RESULTS AND DISCUSSION

The computed glacier areas and volumes are shown in Table 2, together with the detail of the estimations for the different sources of the error in volume. The ice thickness maps are displayed in Figure 2. The individual areas, volumes and average ice thickness lie within 2.6–50.4 km<sup>2</sup>, 0.08–5.54 km<sup>3</sup> and 29–108 m, respectively. The

maximum recorded ice thickness, 265 ± 16 m, corresponds to Fridtjovbreen, which also has the largest average thickness (108 ± 1 m). The total area and volume of the ensemble are 116.06 ± 4.53 km<sup>2</sup> and 10.439 ± 0.373 km<sup>3</sup>, respectively.

The relative errors in volume are generally <10%, except for Aldegondabreen (due to the large GPS error) and Vestre Dahlfonna (due to the large interpolation error compared with its mean thickness). These errors are larger than those usually found in the literature, which we believe are unrealistically small because they are often based on the assumption that all errors are independent.

We have taken RWV to be 170(±2%) m μs<sup>-1</sup> for the time-to-depth conversion, on the basis of field measurements in the region, with the 2% accounting for random errors, because the RWV is known to show both space and time variations, due to changes in material density or water content (Navarro and Eisen, 2010). Both the RWV measurements and the GPR profilings reported in this paper were carried out during early spring, before the onset of surface melting, which minimizes the magnitude of the temporal variations of RWV. Regarding the spatial variations, our analysis shows that, for the glaciers studied and the early springtime, the column-averaged RWVs in the accumulation and ablation zones do not differ substantially. We attribute this to the fact that, despite the higher RWV in firn (~190 m μs<sup>-1</sup>), the firn layer is, in general, not too thick and it is underlain by temperate ice with typical velocities of 165 m μs<sup>-1</sup> or lower, so the column-averaged velocity in the accumulation zone is close to the ~170 m μs<sup>-1</sup> measured at some CMP locations on the upper ablation zone (Jania and others, 2005; Navarro and others, 2005). In addition to random errors, systematic errors could also intervene. The most likely one would be the bias introduced by selecting a constant RWV systematically above (or below) the real values almost everywhere in the glacier. The relative error in volume introduced by a such a hypothetical bias in RWV can be readily estimated: it is equal to the relative error in RWV, because ice thickness is calculated as half the product of two-way travel time and RWV, and volume is computed as area multiplied by thickness.

It is of interest to analyse how well the global and regional volume/area scaling relationships perform for this region. Table 3 summarizes the results of the comparison between



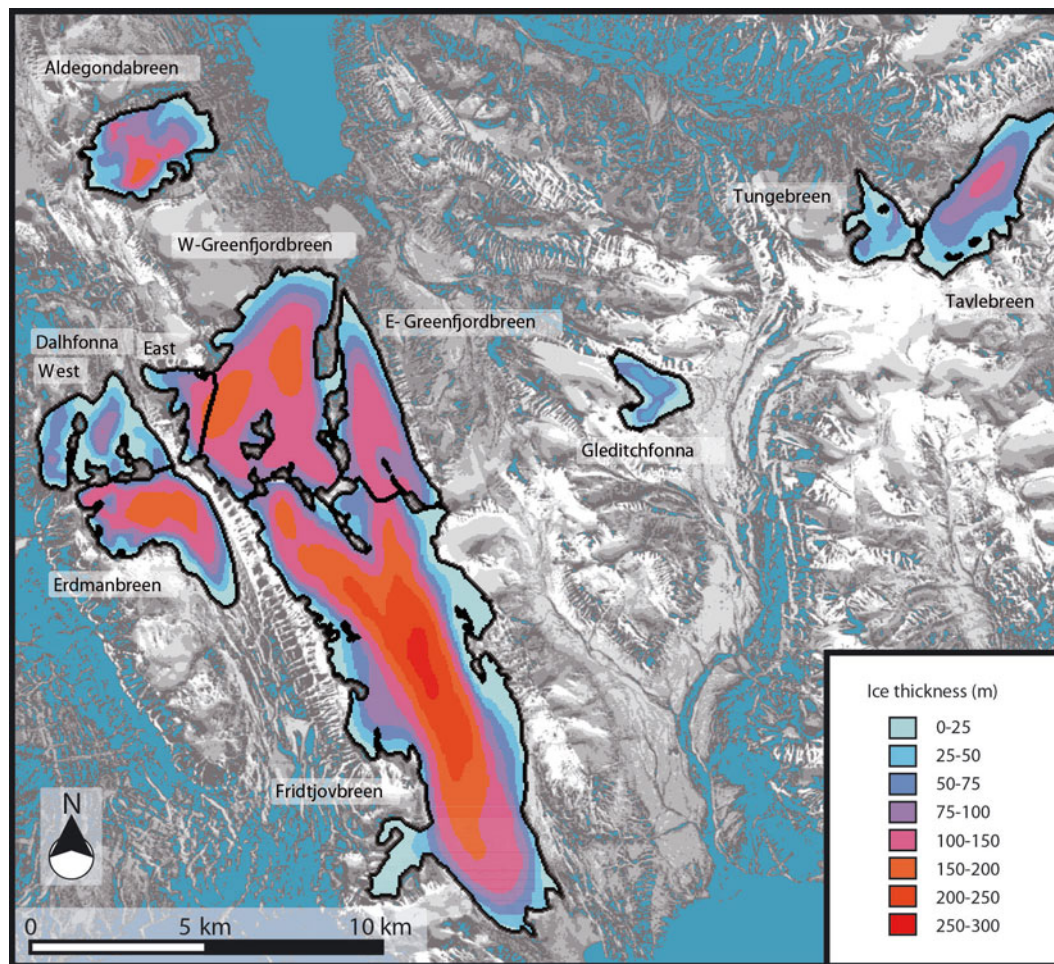


Fig. 2. Ice thickness maps of the studied glaciers.

the measured volumes and those computed from different scaling approaches. As expected, all relationships perform better when applied to the entire set of glaciers rather than to individual glaciers. The largest global discrepancies are those by Hagen and others (1993), in spite of being specific for Svalbard, and by Radić and Hock (2010), which has been

suggested to overestimate the volumes (Grinsted, 2013). At an individual level, the volume overestimate is largest for the thinnest glaciers (Gleditchfonna, Tungebreen and Vestre Dahlfonna). The relationships of Chen and Ohmura (1990) and Bahr and others (1997) give a good overall result and also behave reasonably well at the individual level, while others

Table 3. Comparison of GPR-retrieved volumes,  $V_{GPR}$  ( $\text{km}^3$ ), with volumes computed using area/volume scaling relationships,  $V_{scr}$ , given as per cent differences ( $100 \times (V_{sc} - V_{GPR})/V_{GPR}$ )

Glacier	$V_{GPR}$ $\text{km}^3$	Differences in volume (%)						
		Macheret and Zhuravlev (1982)* %	Hagen and others (1993) <sup>†</sup> %	Bahr and others (1997) <sup>‡</sup> %	Chen and Ohmura (1990) <sup>§</sup> %	Radić and Hock (2010) <sup>¶</sup> %	Grinsted (2013) RGI <sup>  </sup> %	Grinsted (2013) WGI/GLIMS <sup>**</sup> %
Aldegondabreen	0.469	16	38	-14	-12	17	17	5
A. Dahlfonna	0.181	-12	-21	-46	-41	-27	-20	-24
V. Dahlfonna	0.249	108	146	53	58	109	110	88
Erdmanbreen	0.842	-16	4	-35	-34	-12	-13	-23
Fridtjovbreen	5.542	-3	40	3	5	44	23	7
Gleditchfonna	0.076	131	112	44	49	94	111	99
A. Grønfiordbreen	0.637	1	24	-23	-20	7	5	-8
V. Grønfiordbreen	1.918	-16	14	-26	-25	2	-5	-20
Tavlebreen	0.440	41	71	7	9	46	45	28
Tungebreen	0.086	113	99	34	38	81	96	85
Total	10.439	1	35	-7	-5	29	17	2

\*  $V = 0.053A^{1.18}$ . <sup>†</sup>  $V = (33 \ln A + 25)A$ . <sup>‡</sup>  $V = 0.0276A^{1.36}$ . <sup>§</sup>  $V = 0.0285A^{1.357}$ . <sup>¶</sup>  $V = 0.0365A^{1.375}$ . <sup>||</sup>  $V = 0.0433A^{1.29}$ .

\*\*  $V = 0.0540A^{1.20}_{>25 \text{ km}^2}$ ;  $V = 0.0435A^{1.23}_{\leq 25 \text{ km}^2}$ .

producing good results globally show large discrepancies at the individual level (e.g. Macheret and Zhuravlev, 1982). The fact that the Macheret and Zhuravlev (1982) relationship is based on a sample of Svalbard ice masses which includes some glaciers analysed here could explain its good behaviour when applied to our dataset. These results should be treated cautiously, as one of the glaciers, Fridtjovbreen, has a volume nearly as large as the sum of all the others, implying a strong bias. In fact, if this glacier is removed from the dataset, the results change substantially, although Hagen and others (1993) and Radić and Hock (2010) still produce the largest overestimates. Considering both cases (Fridtjovbreen included in and excluded from the dataset), the scaling law by Grinsted (2013) using the World Glacier Inventory (WGI)/Global Land Ice Measurements from Space (GLIMS) inventory gives the best overall result. We note that Fridtjovbreen, in spite of its surge in the 1990s (Murray and others, 2003), does not show an anomalous deviation from the values provided by the area/volume relationships.

Of the glaciers analysed in this paper, volume estimates from ice thickness data retrieved from RES with a dense coverage of the entire glacier surface have only been reported for Aldegondabreen in 1999 (Navarro and others, 2005). The volume reported was  $0.558 \text{ km}^3$ , without an accompanying error estimate. Our present volume estimate, based upon the same GPR field data, is  $\sim 16\%$  smaller. This discrepancy is mostly introduced by the removal, in our volume estimates, of the radar profiles parallel and close to the very steep side-walls of Aldegondabreen. This was recommended by the results of our crossover analysis. Removing such profiles resulted in smaller glacier thickness near both the northern and southern side-walls. In these areas, a large amount of seasonal snow remains accumulated in early spring and, given the high RWV of dry snow (typically  $215\text{--}255 \text{ m } \mu\text{s}^{-1}$ ; e.g. Harper and Bradford, 2003), the glacier thicknesses calculated for these zones by Navarro and others (2005) are expected to be overestimated, leading to a larger total volume. Volume data reported previously for the remaining glaciers analysed in this paper were based either on volume/average thickness relationships (Hagen and others, 1993) or on estimates using airborne RES data along the glacier centre lines and assuming a parabolic shape for the glaciers (Macheret and Zhuravlev, 1980, 1982; Macheret, 1981).

The presence or absence of scattering in the radargrams provides a way to interpret the glacier ice as temperate or cold (Navarro and Eisen, 2010), allowing inference of the hydrothermal structure of the main glaciers of western Nordenskiöld Land. The hydrothermal structure of Fridtjovbreen, prior to its surge in the 1990s (Murray and others, 2003), was interpreted from airborne (Macheret and Zhuravlev, 1980; Dowdeswell and others, 1984a) and ground-based (Glazovskiy and others, 1991) RES data. However, neither the Russian (Macheret and Zhuravlev, 1980, 1982; Macheret, 1981) nor the British (Dowdeswell and others, 1984a,b) echo soundings revealed the polythermal structure of Austre Grønfjordbreen shown in our GPR data. Neither was the Russian airborne echo sounding able to detect the polythermal structure of Aldegondabreen, though it was later inferred from ground-based GPR (Navarro and others, 2005). GPR data from the campaigns from 2010 onwards have revealed the polythermal structure of Tavlebreen (Lavrientiev and others, 2010), Austre and Vestre Grønfjordbreen and Tungebreen (Lavrientiev and others, 2011), as well as the cold structure of Gleditchfonna

(Lavrientiev and others, 2011). GPR data reveal that Erdmanbreen, Austre Dahlfonna and Vestre Dahlfonna are also polythermal.

## CONCLUSIONS

The main conclusions of our analysis are:

The total area and volume of the ensemble of ten western Nordenskiöld Land glaciers considered in this study are  $116.06 \pm 4.53 \text{ km}^2$  and  $10.439 \pm 0.373 \text{ km}^3$ , respectively, while the individual areas, volumes and average ice thickness lie within  $2.6\text{--}50.4 \text{ km}^2$ ,  $0.08\text{--}5.54 \text{ km}^3$  and  $29\text{--}108 \text{ m}$ , respectively. The maximum ice thickness ( $265 \pm 16 \text{ m}$ ) was recorded on Fridtjovbreen.

The total volume of these glaciers calculated using volume/area scaling relationships is overestimated by up to 35% compared to our results. The scaling approach results are biased by the large volume of Fridtjovbreen, which accounts for 45% of the total volume. In general, glaciers with the smallest average ice thickness provide the worst scaling results, with some volumes overestimated by  $>100\%$ .

On the basis of the pattern of scattering in the radargrams, we suggest that Aldegondabreen, Vestre and Austre Dahlfonna, Erdmanbreen, Fridtjovbreen, Vestre and Austre Grønfjordbreen, Tavlebreen and Tungebreen are polythermal glaciers, while Gleditchfonna seems entirely cold.

## ACKNOWLEDGEMENTS

This research was supported by grant EU12009-04096 from the Spanish EuroResearch Programme (a part of the SvalGlaC Project, PolarCLIMATE Programme of the European Science Foundation), grants CTM2008-05878/ANT and CTM2011-28980 from the Spanish National Plan for R&D, and grants 10-05-00133-a and 11-05-00728-a from the Russian Fund of Basic Research. The comments by the Scientific Editor, John Woodward, and an anonymous referee contributed to improve the manuscript.

## REFERENCES

- Arendt A and 77 others (2012) *Randolph Glacier Inventory (RGI), Vers. 1.0: a dataset of Global Glacier Outlines*. Global Land Ice Measurements from Space, Boulder, CO. Digital media: <http://www.glims.org/RGI/randolph.html>
- Bælum K and Benn DI (2011) Thermal structure and drainage system of a small valley glacier (Tellbreen, Svalbard), investigated by ground penetrating radar. *Cryosphere*, **5**(1), 139–149 (doi: 10.5194/tc-5-139-2011)
- Bahr DB, Meier MF and Peckham SD (1997) The physical basis of glacier volume–area scaling. *J. Geophys. Res.*, **102**(B9), 20 355–20 362 (doi: 10.1029/97JB01696)
- Bamber JL, Layberry RL and Gogineni SP (2001) A new ice thickness and bed data set for the Greenland ice sheet. 1. Measurement, data reduction, and errors. *J. Geophys. Res.*, **106**(D24), 33 773–33 780 (doi: 10.1029/2001JD900054)
- Berikashvili V, Vasilenko E, Macheret YuYa and Sokolov VG (2006) Ul'sny radar dlya zondirovaniya lednikov s opticheskim kanalom sinkhronizatsii i tifrovoy brabotkoy signalov [Monopulse radar for sounding of glaciers with optical synchronization channel and digital processing of signals]. *Radiotekhnika*, **9**, 52–57



- Bohorquez P and Darby SE (2008) The use of one- and two-dimensional hydraulic modelling to reconstruct a glacial outburst flood in a steep Alpine valley. *J. Hydrol.*, **361**(3–4), 240–261 (doi: 10.1016/j.jhydrol.2008.07.043)
- Chen J and Ohmura A (1990) Estimation of Alpine glacier water resources and their change since the 1870s. *IAHS Publ.* 193 (Symposium at Lausanne 1990 – *Hydrology in Mountainous Regions*), 127–135
- Cuffey KM and Paterson WSB (2010) *The physics of glaciers*, 4th edn. Butterworth-Heinemann, Oxford
- D'Errico J (2006) *Surface fitting using gridfit*. MATLAB Central File Exchange <http://www.mathworks.es/matlabcentral/fileexchange/8998-surface-fitting-using-gridfit>
- Davis BM (1987) Uses and abuses of cross-validation in geostatistics. *Math. Geol.*, **19**(3), 241–248
- Dowdeswell JA, Drewry DJ, Liestøl O and Orheim O (1984a) Radio-echo sounding of Spitsbergen glaciers: problems in the interpretation of layer and bottom returns. *J. Glaciol.*, **30**(104), 16–21
- Dowdeswell JA, Drewry DJ, Liestøl O and Orheim O (1984b) Airborne radio echo sounding of sub-polar glaciers in Spitsbergen. *Nor. Polarinst. Skr.* 182
- Glazovskiy AF, Macheret Y, Moskalevskiy MY and Jania J (1991) Tidewater glaciers of Spitsbergen. *IAHS Publ.* 208 (Symposium at St Petersburg 1990 – *Glaciers–Ocean–Atmosphere Interactions*), 229–239
- Grinsted A (2013) An estimate of global glacier volume. *Cryosphere*, **7**(1), 141–151 (doi: 10.5194/tc-7-141-2013)
- Hagen JO, Liestøl O, Roland E and Jørgensen T (1993) Glacier atlas of Svalbard and Jan Mayen. *Nor. Polarinst. Medd.* 129
- Hagen JO, Melvold K, Pinglot F and Dowdeswell JA (2003) On the net mass balance of the glaciers and ice caps in Svalbard, Norwegian Arctic. *Arct. Antarct. Alp. Res.*, **35**(2), 264–270
- Harper JT and Bradford JH (2003) Snow stratigraphy over a uniform depositional surface: spatial variability and measurement tools. *Cold Reg. Sci. Technol.*, **37**(3), 289–298 (doi: 10.1016/S0165-232X(03)00071-5)
- Huss M and Farinotti D (2012) Distributed ice thickness and volume of all glaciers around the globe. *J. Geophys. Res.*, **117**(F4), F04010 (doi: 10.1029/2012JF002523)
- Isaaks EH and Srivastava RM (1989) *An introduction to applied geostatistics*. Oxford University Press, New York
- Jania J and 9 others (2005) Temporal changes in the radiophysical properties of a polythermal glacier in Spitsbergen. *Ann. Glaciol.*, **42**, 125–134 (doi: 10.3189/172756405781812754)
- König M, Nuth C, Kohler J, Moholdt G and Pettersen R (in press) A digital glacier database for Svalbard. In Kargel JS, Leonard GJ, Bishop MP, Käab A and Raup BH eds. *Global Land Ice Measurements from Space*. Praxis-Springer, Chichester, **10**, 230–239
- Kulnitsky LM, Gofman PA and Tokarev MY (2000) Matematicheskaya obrabotka dannykh georadiolokatsii i sistema RADEXPRO [Mathematical processing of georadar data and RADEXPRO system]. *Razv. Okhrana Nedr*, **3**, 6–11
- Lavrientiev II, Macheret YuYa, Holmlund P and Glazovsky AF (2010) Thermal structure and subglacial drainage system of Tavleebreen, Svalbard. In *Abstract: International Polar Year, Oslo Science Conference, 8–12 June 2010, Oslo, Norway*
- Lavrientiev II, Macheret YuYa and Glazovsky AF (2011) Stroyeniye i gidrotermicheskaya struktura lednikov Shpitsbergena na Zemle Nordenshel'da po dannym radiozondirovaniya [Configuration and hydrothermal structure of Svalbard glaciers on Nordenskiöld Land by radio-echo sounding data.] In *Abstracts of Conference on Integrated and Interdisciplinary Research in Polar Regions, 3–8 October 2011, Sochi, Russia*. Scientific Council on Arctic and Antarctic Research, Russian Academy of Sciences, Moscow, (1981) Forms of glacial relief of Spitsbergen glaciers. *Ann. Glaciol.*, **2**, 45–51
- Macheret Y and Zhuravlev AB (1980) Radiolokatsionnoye zondirovaniye lednikov Shpitsbergena s vertoleta [Radio echo-sounding of Spitsbergen's glaciers from a helicopter]. *Mater. Glyatsiol. Issled./Data Glaciol. Stud.* **37**, 109–131 [in Russian with English summary]
- Macheret YuYa and Zhuravlev AB (1982) Radio echo-sounding of Svalbard glaciers. *J. Glaciol.*, **28**(99), 295–314
- Macheret YuYa, Moskalevskiy MY and Vasilenko EV (1993) Velocity of radio waves in glaciers as an indicator of their hydrothermal state, structure and regime. *J. Glaciol.*, **39**(132), 373–384
- Murray T, Luckman A, Strozzi T and Nuttall A-M (2003) The initiation of glacier surging at Fridtjovbreen, Svalbard. *Ann. Glaciol.*, **36**, 110–116 (doi: 10.3189/172756403781816275)
- Navarro F and Eisen O (2010) Ground-penetrating radar in glaciological applications. In Pellikka P and Reese WG eds. *Remote sensing of glaciers: techniques for topographic, spatial and thematic mapping of glaciers*. Taylor & Francis, London, 195–229
- Navarro FJ, Glazovsky AF, Macheret YuYa, Vasilenko EV, Corcuera MI and Cuadrado ML (2005) Ice-volume changes (1936–1990) and structure of Aldegondabreen, Spitsbergen. *Ann. Glaciol.*, **42**, 158–162 (doi: 10.3189/172756405781812646)
- Parkinson BW, Spilker JJ, Axelrad P and Enge P (1996) *Global Positioning System: theory and applications*, Vol. 2. American Institute of Aeronautics and Astronautics, Reston, VA
- Radić V and Hock R (2010) Regional and global volumes of glaciers derived from statistical upscaling of glacier inventory data. *J. Geophys. Res.*, **115**(F1), F01010 (doi: 10.1029/2009JF001373)
- Radić V and Hock R (2011) Regionally differentiated contribution of mountain glaciers and ice caps to future sea-level rise. *Nature Geosci.*, **4**(2), 91–94 (doi: 10.1038/ngeo1052)
- Retzlaff R, Lord N and Bentley CR (1993) Airborne-radar studies: Ice Streams A, B and C, West Antarctica. *J. Glaciol.*, **39**(133), 495–506
- Rignot E, Velicogna I, Van den Broeke MR, Monaghan A and Lenaerts J (2011) Acceleration of the contribution of the Greenland and Antarctic ice sheets to sea level rise. *Geophys. Res. Lett.*, **38**(5), L05503 (doi: 10.1029/2011GL046583)
- Saintenoy A and 7 others (2013) Deriving ice thickness, glacier volume and bedrock morphology of Austre Lovénbreen (Svalbard) using GPR. *Near Surf. Geophys.*, **11**(2), 253–261 (doi: 10.3997/1873-0604.2012040)
- Sharma S and Banerjee P (2009) Effect of errors in position coordinates of the receiving antenna on single satellite GPS timing. In *2009 Joint Meeting of the European Frequency and Time Forum and the IEEE International Frequency Control Symposium, 20–24 April 2009, Besançon, France*. Institute of Electrical and Electronics Engineers, Piscataway, NJ, 695–699
- Solomon S and 7 others eds. (2007) *Climate change 2007: the physical science basis. Contribution of Working Group I to the Fourth Assessment Report of the Intergovernmental Panel on Climate Change*. Cambridge University Press, Cambridge
- Vasilenko EV, Sokolov VA, Macheret YuYa, Glazovsky AF, Cuadrado ML and Navarro FJ (2002) A digital recording system for radioglaciological studies. *Bull. R. Soc. N. Z.*, **35**, 611–618
- Vasilenko E, Glazovsky A, Lavrentiev I, Macheret YuYa and Navarro FJ (2006) Izmeneniya tolshchiny i gidrotermicheskoy struktury lednika Frit'of s 1977 po 2005 god [Changes in ice thickness and hydrothermal structure of Fridtjovbreen in 1977–2005]. *Mater. Glyatsiol. Issled./Data Glaciol. Stud.* **101**, 157–162
- Vasilenko EV, Machío F, Lapazaran JJ, Navarro FJ and Frolovskiy K (2011) A compact lightweight multipurpose ground-penetrating radar for glaciological applications. *J. Glaciol.*, **57**(206), 1113–1118 (doi: 10.3189/002214311798843430)